Electronic Supplementary Information

Secondary dialkylammonium salt/crown ether [2]pseudorotaxanes as nanostructuring platforms for proton transport

Lijie Li,[a] Lipeng He,[a] Binghua Wang,[b] Peng Ge,[c] Lei Jing,[c] Haomin Liu,[a] Chenliang Gong,[a] Bin Zhang,*[b] Junhu Zhang,*[c] and Weifeng Bu *[a]

[a] *Key Laboratory of Nonferrous Metals Chemistry and Resources Utilization of Gansu Province, State Key Laboratory of Applied Organic Chemistry, and College of Chemistry and Chemical Engineering, Lanzhou University, Lanzhou, 730000 (China), E-mail: buwf@lzu.edu.cn*
[b] *School of Materials Science & Engineering, Zhengzhou University, Zhengzhou, 450002 (China), E-mail: binzhang@zzu.edu.cn*
[c] *State Key Laboratory of Supramolecular Structure and Materials, College of Chemistry, Jilin University, Changchun, 130012 (China), E-mail: zjh@jlu.edu.cn*

Instruments and Materials

All solvents and reagents were purchased commercially with reagent grade quality. ^{1}H and ^{13}C NMR spectra were recorded on a JNM-ECS400 spectrometer, performing in CDCl$_3$ solutions and using TMS as an internal standard. Electrospray ionization mass spectra (ESI-MS) were performed with Bruker microTOF-Q II. Fourier transformation infrared (FT-IR) spectra were obtained on a Nicolet NEXUS 670 spectrometer with a resolution of 4 cm^{-1}. The samples were compressed into KBr thin slices. Gel permeation chromatography (GPC) plots were recorded on a Shimadzu LC-20AD instrument with a calibration standard of polystyrene and an eluent solvent of tetrahydrofuran (THF). C, H, and N elemental analyses were obtained with Elementar Analysensysteme GmbH VarioEL element analyzer(Germany), while for Mo and W elements, the data were achieved on a Analytikjena PQ 9000 inductively coupled plasma atomic emission spectrometer. The proton conductivity (σ) was measured on an Eco Chemie B.V Autolab (PGSTAT30) electrochemical workstation by an AC impedance method with two platinum wire electrodes (Φ 0.5 × 37 mm) or two round flat copper electrodes (Φ 0.6 cm) over a frequency range from 0.1 Hz to 100 kHz. The samples were made into a rectangle between two platinum electrodes or between two round flat copper electrodes, which were further immersed in deionized water during measurements. The σ value was calculated by the following equation: $\sigma = L/RS$, where L (cm) is the distance between two electrodes (the thickness of sample), R (Ω) is the sample resistance, and S (cm^2) is the cross-sectional area of the electrodes. SEM images were obtained with JSM-5600LV. AFM measurements were carried out using a Dimension

Icon microscope from Bruker. AFM samples were obtained on p-doped silicon wafers (resistivity: 0.001–0.0012 Ω cm). Images of both surface topography and electrical conductivity were recorded by using PeakForce TUNA mode under ambient conditions. Small-angle X-ray scattering (SAXS) and wide-angle X-ray scattering (WAXS) experiments were simultaneously performed on a Nano-inXider ($\lambda = 0.154$ nm, Xenocs, France). All measurements were carried out at room temperature. All water- and air-sensitive reactions were carried out under argon atmosphere.

Synthetic Procedures and Characterization Details.

4.1.5.2,5,8,11,18,21,24,27-Octaoxa-tricyclo[26.4.0.0^{12,17}]-dotriaconta-1(28),12,14,16,29,31-hexaene-14-carboxylic acid (**24C8-COOH**) was synthesized according to the procedures in the related literature[S1] and showed identical ^{1}H NMR spectra to those reported therein. **PCL-DBA**[S2] was synthesized according to the procedures in the related literature and showed identical ^{1}H NMR spectra and GPC to those reported therein.

***N,N*-dimethyldodecyl-12-dodecanolammonium bromide (C-Cation)**: Into a 100 mL schlenk tube were added 12-bromododecanol (6.0 mmol, 1.59 g). Then, 20 mL EtOH and *N,N*-dimethyldodecylamine (5.0 mmol, 1.06 g) were added successively. The resulting mixture was further stirred at 80 °C for 3 d. After removal of the solvents, the product was precipitated from diethyl ether, which was filtered off and washed diethyl ether. The product was a white solid (2.09 g, 88% yield). ^{1}H NMR (400 MHz, CDCl$_3$), δ: 3.36-3.62 (m, 2H), 3.55-3.48 (m, 4H), 3.40 (s, 6H), 1.71-1.53 (m, 6H), 1.42-1.25 (m, 34H), 0.88 (t, J = 4.0 Hz, 3H). ^{13}C NMR (100 MHz, CDCl$_3$), δ: 77.32, 77.00, 77.68, 63.82, 62.84, 51.23, 32.67, 31.85, 29.54, 29.41, 29.35, 29.33, 29.27, 29.24, 29.22, 29.19, 29.06, 26.21, 26.16, 25.63, 22.75, 22.63, 14.08. HRMS (m/z), [M–Br]$^+$ calculated: 398.4356, found: 398.4353.

C-DB24C8: Into a 50 mL round-bottle flask with 20 mL dichloromethane (DCM) were added **DB24C8-COOH** (2.7 mmol, 1.32 g), **C-Cation** (2.7 mmol, 1.28 g), and 4-dimethylaminopyridine (DMAP) (2.7 mmol, 134 mg). This mixture was stirred in an ice-bath for 10 min and then 1-(3-dimethylaminopropyl)-3-ethylcarbodiimide hydrochloride (**EDC**) (5.4 mmol, 1.04 g) was added. The resulting mixture was warmed to room temperature and stirred for 24 h. The reaction was monitored by TLC and stopped until the reactants disappeared completely. After evaporating the solvent, the crude product was purified by column chromatography (silica gel) using dichloromethane and methanol (5:1) as eluent. A faint yellow solid was obtained (2.34g, 91% yield). ^{1}H NMR (400 MHz, CDCl$_3$), δ: 7.64 (dd, J_1 = 8.4 Hz, J_2 = 1.6 Hz, 1H), 7.51 (d, J = 1.6 Hz, 1H), 6.88-6.83 (m, 5H), 4.26 (t, J = 6.8 Hz, 2H), 4.17 (dt, J_1 = 16.7 Hz, J_2 = 4.1 Hz, 8H), 3.95-3.90 (m, 8H), 3.83 (d, J = 2.0 Hz, 8H), 3.51-3.47 (m, 4H), 3.39 (s, 6H), 1.75-1.69 (m, 6H), 1.42-1.25 (m, 34H), 0.87 (t, J = 6.8 Hz, 3H). ^{13}C NMR (100 MHz, CDCl$_3$, δ): 166.32, 152.63, 148.69, 148.02, 123.74, 123.08, 121.32, 114.19, 113.82, 111.84, 77.32, 77.00, 76.68, 71.29, 71.19, 71.11, 69.80, 69.65, 69.50, 69.34, 69.20, 69.15, 69.11, 64.87, 63.69, 51.18, 31.79, 29.48, 29.36, 29.27, 29.23, 29.12, 28.62, 26.14, 25.89, 22.68, 22.58, 14.05, 0.92. HRMS (m/z), [M–Br]$^+$ calculated: 872.6246, found: 872.6249.

Mo$_{132}$-DB24C8: $(NH_4)_{42}[Mo_{132}O_{372}(CH_3COO)_{30}(H_2O)_{72}] \cdot 300H_2O \cdot 10CH_3COONH_4$ (234 mg, 0.008 mmol) was dissolved in water (50 mL) to give a dark brown solution. This solution was added into a

chloroform solution of **C-DB24C8** (300 mg, 0.315 mmol, 50 mL) with vigorous stirring for 1 h at room temperature. Then, the chloroform phase was separated and further extracted by dichloromethane (3 × 25 mL). The organic layers were merged and the solvents were removed under reduced pressure (431 mg, yield 92 %). Elemental analysis calcd (%) for (C-DB24C8)$_{40}$(NH$_4$)$_2$[Mo$_{132}$O$_{372}$(CH$_3$COO)$_{30}$(H$_2$O)$_{72}$] (M = 56652.16 g/moL): C 44.52, H 6.55, N 1.04, Mo 22.67; found: C 44.19, H 6.29, N 0.88, Mo 22.36.

W$_{12}$-DB24C8 was similarly prepared for **Mo$_{132}$-DB24C8**, but with K$_4$[SiW$_{12}$O$_{40}$]·30H$_2$O as a reactant. Elemental analysis calcd (%) for (C-DB24C8)$_4$[SiW$_{12}$O$_{40}$] (M = 6367.06 g/moL^{-1}): C 38.48, H 5.45, N 0.88, W 34.65; found: C 38.24, H 5.05, N 0.71, W 30.63.
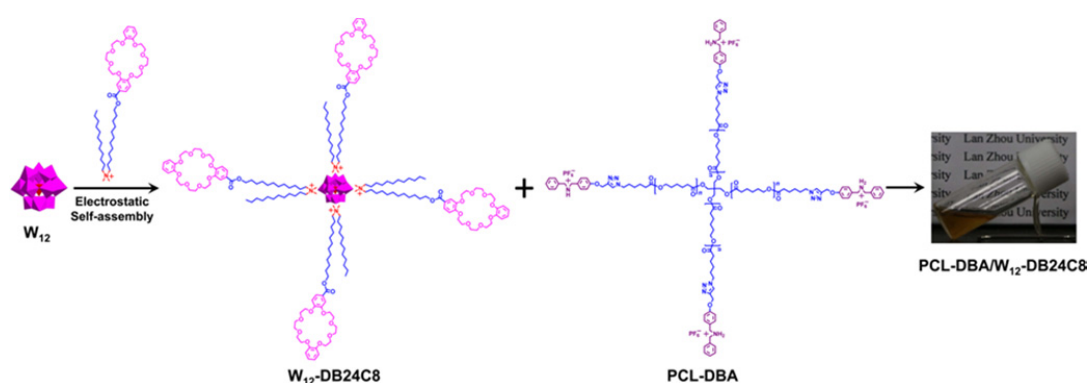
Fig. S1 The polyoxometalate cluster of **W$_{12}$** was encapsulated by the cationic surfactant with a DB24C8 group. The resulting encapsulated complex bearing 4 DB24C8 groups cross-linked **PCL-DBA** stars to form supramolecular hybrid organogel as a result of the DBA/DB24C8 [2]pseudorotaxane connection.

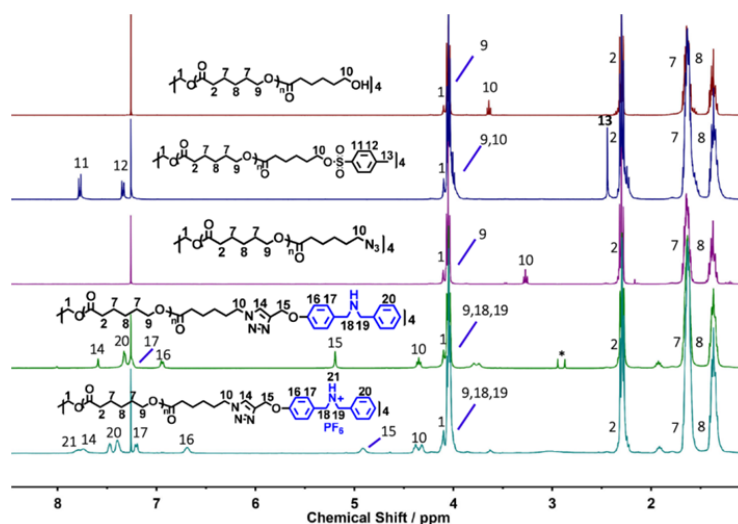**Fig. S2** ^{1}H NMR spectrum of (a) **PCL-OH**, (b) **PCL-OTs**, (c) **PCL-N$_3$**, and (d) **PCL-Amine**, (e) **PCL-DBA** in CDCl$_3$.

Table S1. GPC values of **PCL-OH**, **PCL-OTs**, **PCL-N₃**, **PCL-Amine**, **PCL-DBA**.

	M_n	PDI
PCL-OH	10.3 KDa	$M_w/M_n = 1.13$
PCL-OTs	10.6 KDa	$M_w/M_n = 1.10$
PCL-N₃	10.3 KDa	$M_w/M_n = 1.11$
PCL-Amine	12.7 KDa	$M_w/M_n = 1.15$
PCL-DBA	10.0 KDa	$M_w/M_n = 1.03$
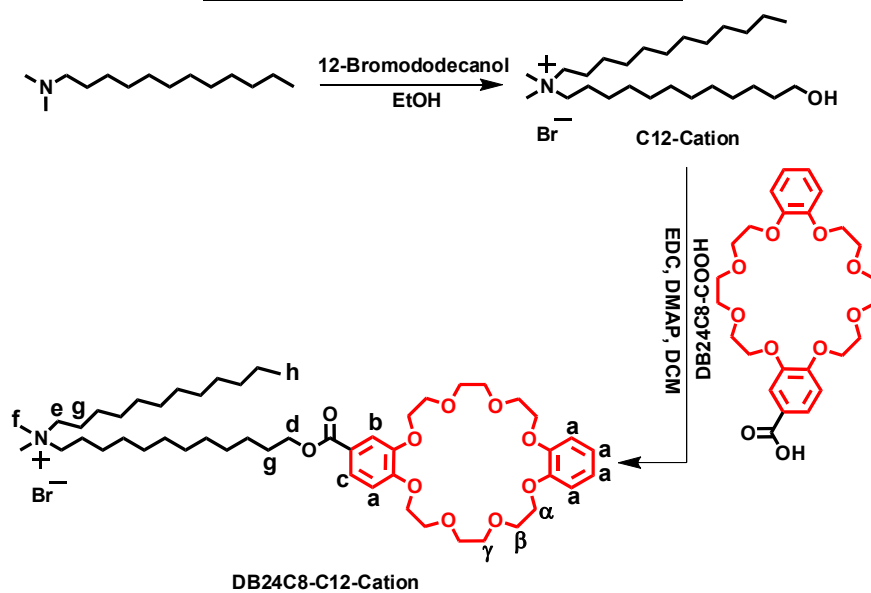
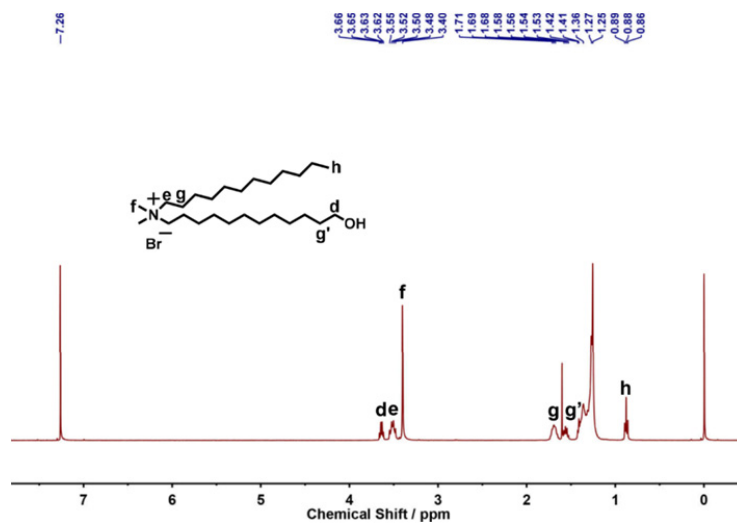**Fig. S3** The synthetic procedure of the cationic surfactant bearing a DB24C8 group (**C-DB24C8**).

Fig. S4 ¹H NMR spectrum of **C-Cation** in CDCl₃.
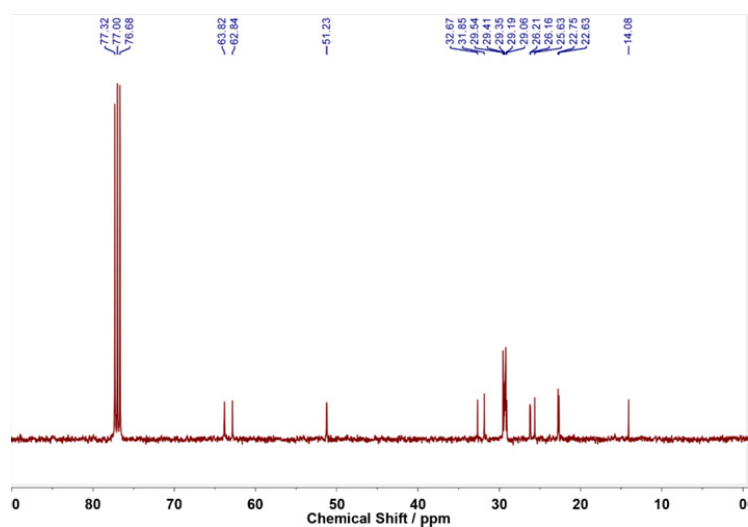
Fig. S5 ^{13}C NMR spectrum of **C-Cation** in CDCl$_3$.
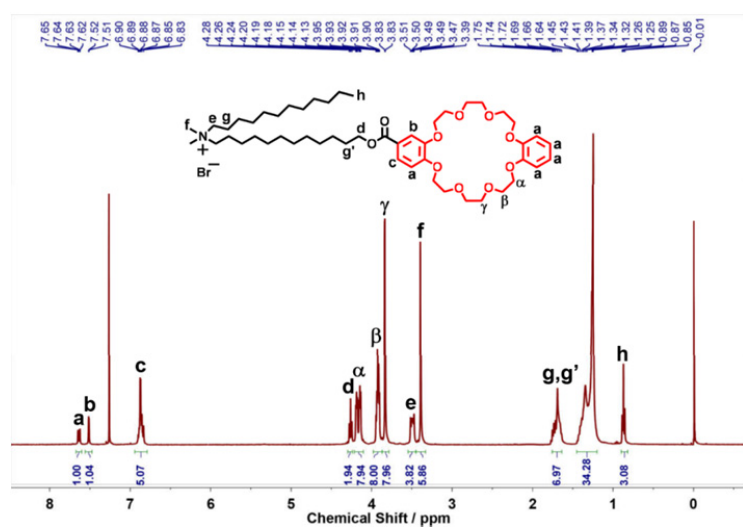
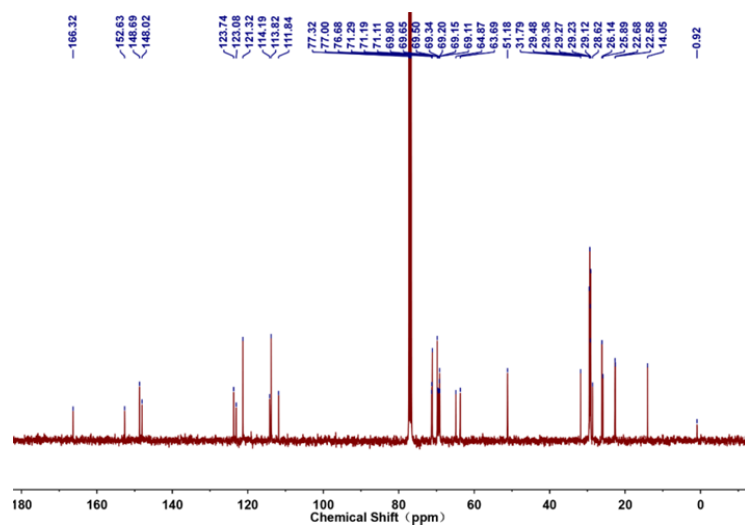**Fig. S6** ^{1}H NMR spectrum of **C-DB24C8** in CDCl$_3$.

Fig. S7 ^{13}C NMR spectrum of **C-DB24C8** in CDCl$_3$.
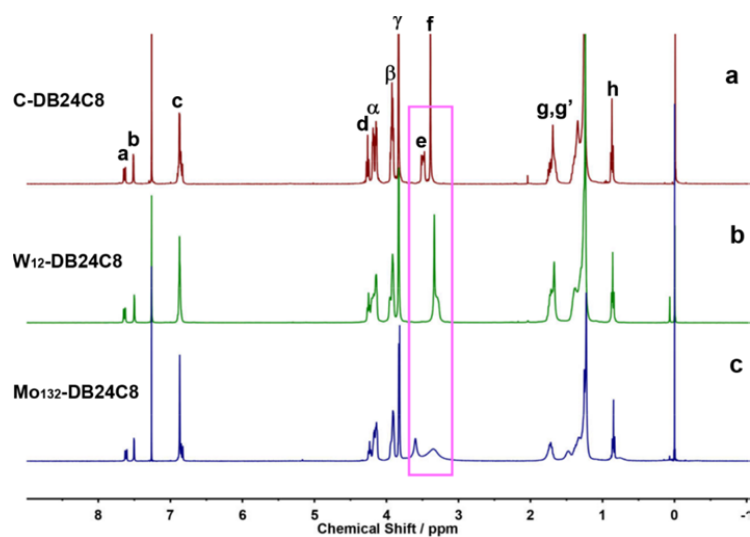
Fig. S8 ^{1}H NMR spectrum of (a) **C-DB24C8**, (b) **W$_{12}$-DB24C8** and (c) **Mo$_{132}$-DB24C8** in CDCl$_3$.
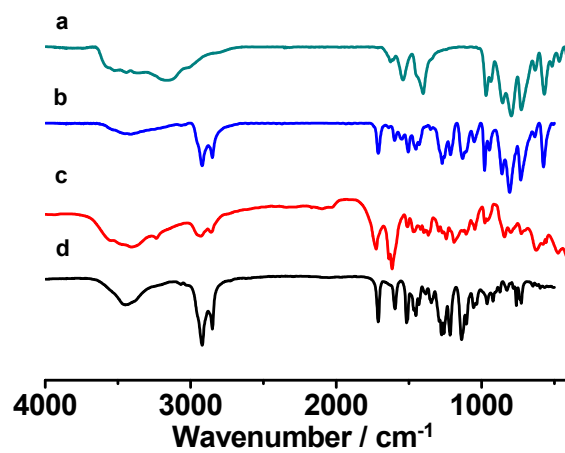
Fig. S9 FT-IR spectra spectra of (a) **Mo$_{132}$**, (b) **Mo$_{132}$-DB24C8**, (c) **Mo$_{132}$-PCL** and (d) **C-DB24C8**.
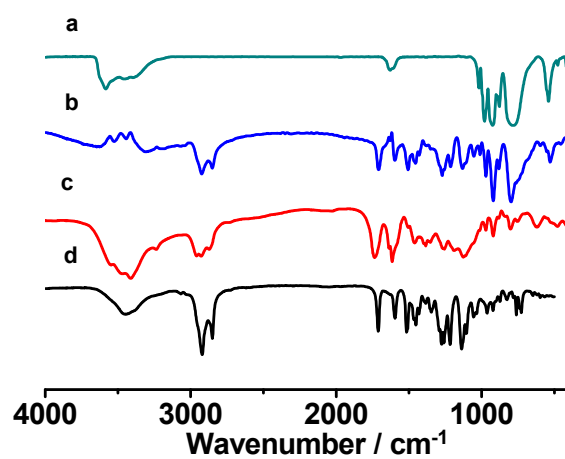
Fig. S10 FT-IR spectra of (a) **W$_{12}$**, (b) **W$_{12}$-DB24C8**, (c) **W$_{12}$-PCL** and (d) **C-DB24C8**.
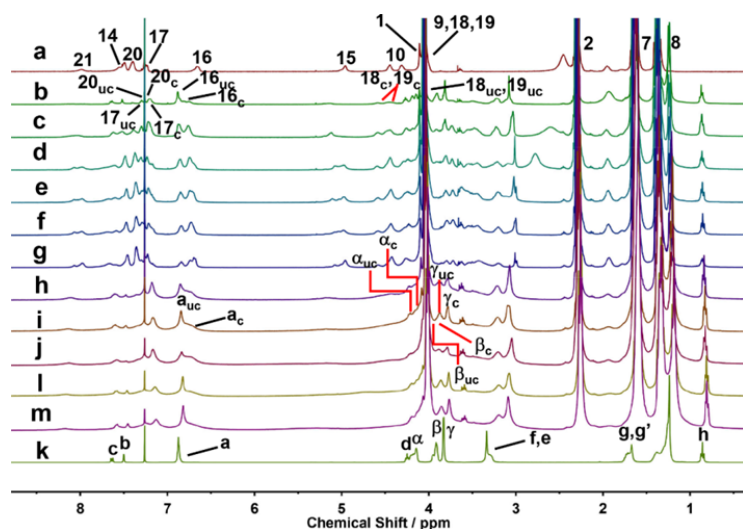
Fig. S11 ^{1}H NMR spectra (400 MHz) of PCL-DBA (a) and (k) W_{12}-DB24C8 in CDCl$_3$. Concentration-dependent ^{1}H NMR spectra of the mixture of W_{12}-DB24C8 with 4 equivalents of PCL-DBA in CDCl$_3$. The molar ratio of DB24C8 and DBA groups was 1:1. The concentration of W_{12}-DB24C8 was (b) 1.0 mM, (c) 2.0 mM, (d) 3.0 mM, (e) 4.0 mM, (f) 5.0 mM, (g) 7.0 mM, (h) 9.0 mM, (i) 12 mM, (j) 15 Mm, (l) 18 mM, and (m) 21 mM. Here, "U" and "C" denote uncomplexed and complexe moieties, respectively.
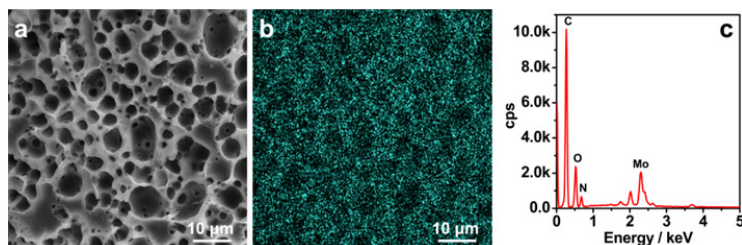

Fig. S12 The SEM image of the dried organogel of **Mo$_{132}$-PCL** (a) and its EDX element mapping of molybdenum (b and c).
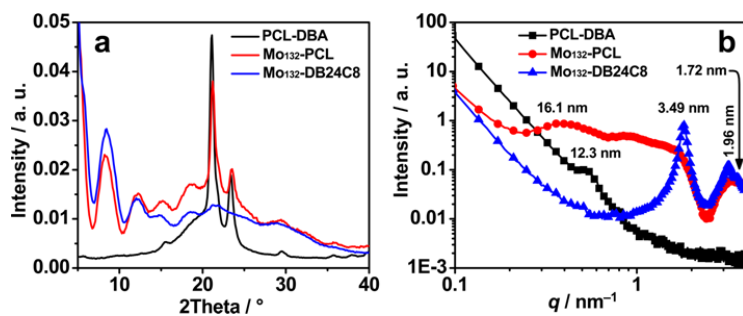

Fig. S13 WAXS (a) and SAXS patterns (b) of **PCL-DBA**, **Mo$_{132}$-PCL**, and **Mo$_{132}$-DB24C8**.
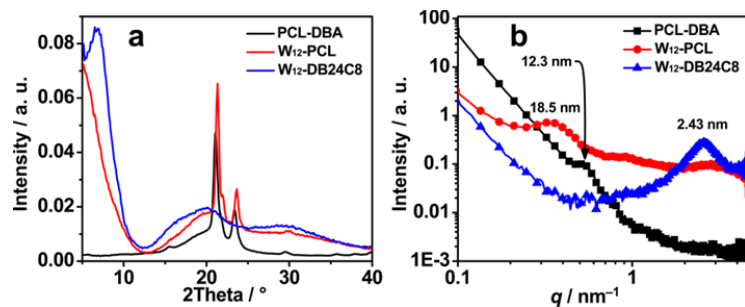
Fig. S14 WAXS (a) and SAXS patterns (b) of **PCL-DBA**, W_{12}-**PCL**, and W_{12}-**DB24C8**.
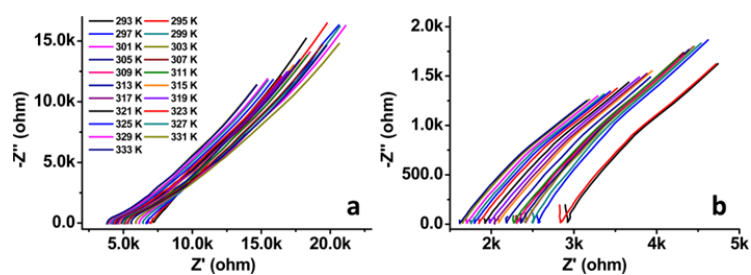
Fig. S15 Nyquist plots of Mo_{132}-**PCL** (a) and W_{12}-**PCL** (b) at different temperatures.
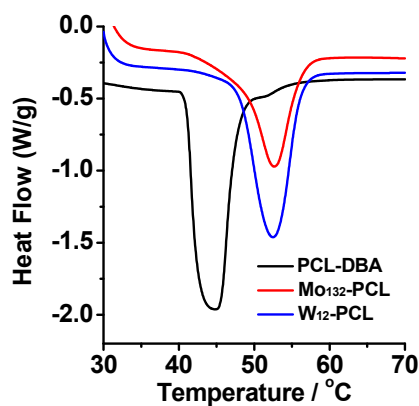
Fig. S16 DSC curves of **PCL-DBA**, Mo_{132}-**PCL**, and W_{12}-**PCL**.
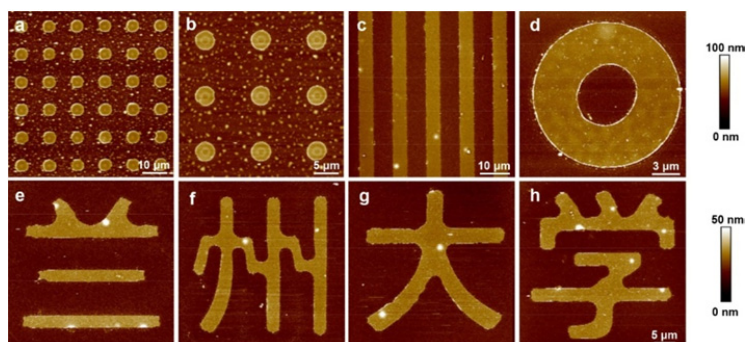
Fig. S17 Topographic AFM images of Mo_{132}-PCL in different microscopic shapes (a-d) and Chinese characters (e-h, Lanzhou University) prepared by soft lithography technique.
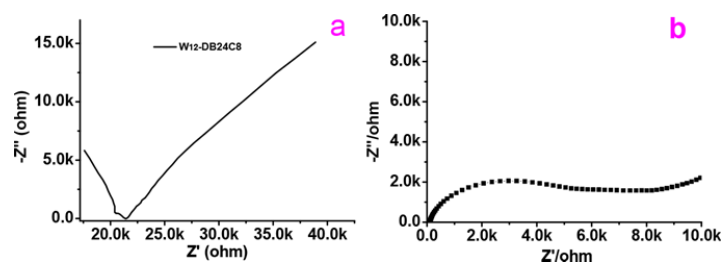
Fig. S18 Nyquist plots of **W_{12}-DB24C8** (a) and **Mo_{132}-DB24C8** (b) at room temperatures.
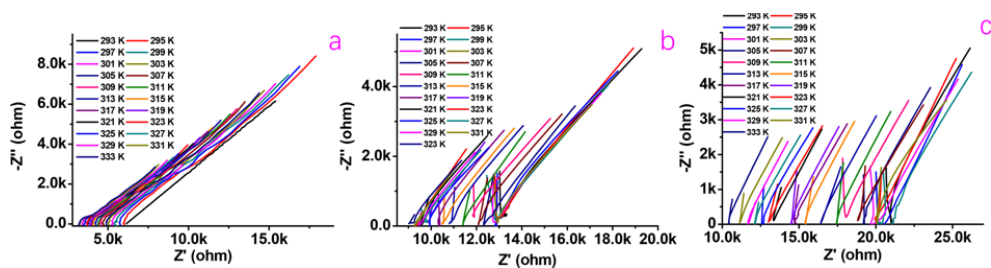
Fig. S19 Nyquist plots of (a, 0.5 eq **Mo_{132}-DB24C8**, 0.5 eq **W_{12}-DB24C8**, 1 eq **PCL**, **0.5-0.5-1**), (b, 1 eq **Mo_{132}-DB24C8**, 2 eq **PCL**, **1-2**), and (c, 1 eq **Mo_{132}-DB24C8**, 3 eq **PCL**, **1-3**).

Fig. S20 To strengthen the rational control of proton conductivity, we have further prepared three additional supramolecular networks at different mo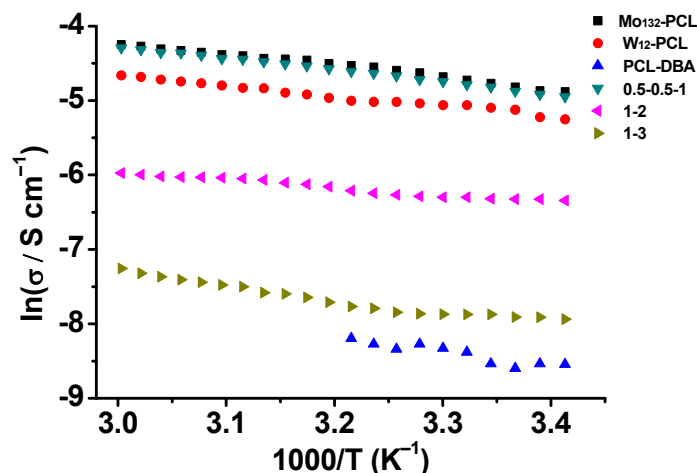lar ratios (0.5 eq **Mo₁₃₂-DB24C8**, 0.5 eq **W₁₂-DB24C8**, 1 eq **PCL**, **0.5-0.5-1**), (1 eq **Mo₁₃₂-DB24C8**, 2 eq **PCL**, **1-2**), and (1 eq **Mo₁₃₂-DB24C8**, 3 eq **PCL**, **1-3**). As shown in Fig. S19, the supramolecular network of **0.5-0.5-1** showed the intermediate σ values between **Mo₁₃₂-PCL** and **W₁₂-PCL**. With increasing contents of **PCL-DBA**, the supramolecular networks showed a significant decrease in the σ values, for example, in the case **1-2** and **1-3**. These results can be expected definitely. It was therefore concluded that the rational control of proton conductivity can be realized by precisely controlling the number or density of the [2]pseudorotaxanes from DBA salts and DB24C8 groups in the supramolecular networks.
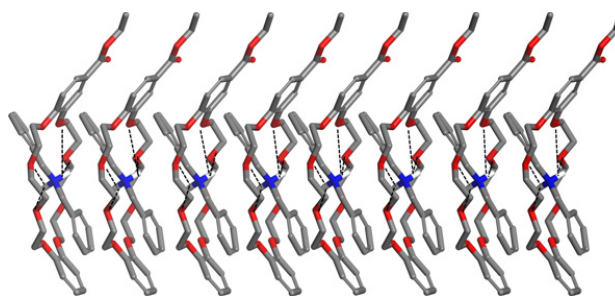
Fig. S21 The cartoon representation for protons by forming a hydrogen-bonding network to pass through the channels in the cases of **Mo₁₃₂-PCL** and **W₁₂-PCL**. Actually, the distance between the secondary dialkylammonium salt/crown ether [2]pseudorotaxanes is believed to be rather small, as inferred from the crystalline PCL arms (Fig. S13 and S14). In Fig. 1, the large distance was demonstrated between the secondary dialkylammonium salt/crown ether [2]pseudorotaxanes, which was only for clarity.

Results and Discussion

As revealed in the ^{1}H NMR spectra of Figure S5 and S6, the proton signals of H_e (*N-CH${}_3$*) and H_f (*N-CH${}_2$*) of both **Mo${}_{132}$-DB24C8** and **W${}_{12}$-DB24C8** showed significant broadening, indicating the limited mobility of the cationic head of **C-DB24C8**. This was accordingly due to strong electrostatic interactions between the cationic head of **C-DB24C8** and clusters of **Mo${}_{132}$** or **W${}_{12}$** in the surfactant-encapsulated clusters.

For **Mo${}_{132}$-DB24C8** and **Mo${}_{132}$-PCL**, the characteristic absorption bands of **Mo${}_{132}$** appeared in their FT-IR spectra of 979, 946, 860, 807, and 731 cm^{-1} (Fig. S9), while for **C-DB24C8**, v_{as} and v_s (CH${}_2$) bands appeared at 2921 and 2850 cm^{-1}, respectively (Fig. S9). These results indicated that **C-DB24C8** was attached to the surface of **Mo${}_{132}$** and its metal-oxygen framework was well retained. For **W${}_{12}$-DB24C8** and **W${}_{12}$-PCL**, W=O, Si-O, W-O-W, v_{as}, and v_s (CH${}_2$) characteristic bands appeared at 966, 923, 803, 2922, and 2851 cm^{-1}, respectively (Fig. S10).

In this work, percentage recognition (*p*) is fraction of the DBA moieties bound into the DB24C8 groups.[6f] The *p* values was calculated as follows: Three broad resonances were clearly observed at δ = 4.37, 4.49, and 4.57 ppm (Fig. 2a, b, and k). With reference to previous ^{1}H NMR studies on host−guest recognition between DB24C8 and DBA groups, these three resonance signals were definitely assigned to the benzylic methylene protons (H_{18C} + H_{19C}) adjacent to the NH${}_2^+$ centers interpenetrated fully by the DB24C8 moieties. The resonance signals of the uncomplexed benzylic methylene protons (H_{18UC} + H_{19UC}) cannot be clearly assigned because of the highly overlapping resonances with H_9. The individual proton signal of H_C at 7.64 ppm could be clearly assigned at 0.1, 0.2, and 0.3 mM. This proton signal together with the total (H_{18C} + H_{19C}) signals could be used as a standard to calculate the *p* values: $p = A(H_{18C}+H_{19C})/4AH_C$, in which $A(H_{18C}+H_{19C})$ and AH_C are the average intergrals of ($H_{18C}+H_{19C}$) and H_C, respectively. Accordingly, the *p* values were determined to be 92.5%, 94.5%, and 96.5% at the concentrations of 0.1, 0.2, and 0.3 mM, respectively.

The cationic surfactant bearing a DB24C8 group occupied a length of 3.3 nm, as estimated by the Corey-Pauling-Koltun (CPK) model. The alkyl chains adopted an all-trans conformation. This value together with the diameters of **Mo${}_{132}$** (2.8 nm) and **W${}_{12}$** (1.0 nm) yielded total sizes of 9.4 and 7.6 nm for **Mo${}_{132}$-DB24C8** and **W${}_{12}$-DB24C8**, respectively. These values were much larger than the sizes obtained from the SAXS experiments for **Mo${}_{132}$-DB24C8** (4.0 nm) and **W${}_{12}$-DB24C8** (2.4 nm).

On the other hand, the clusters of **Mo${}_{132}$** and **W${}_{12}$** have surface areas of 33.4 and 3.14 nm^2, respectively.[S3] Therefore, the cationic headgroup areas were estimated to be 0.84 and 0.78 nm^2 in the cases of **Mo${}_{132}$-DB24C8** and **W${}_{12}$-DB24C8**, respectively. These values were larger than those areas of alkyltrimethylammonium (ca. 0.6 nm^2) and alkyl chains (ca. 0.2 nm^2). Moreover, in the starlike hybrids of **Mo${}_{132}$-DB24C8** and **W${}_{12}$-DB24C8**, the surfactant molecules were radiated from the clusters of **Mo${}_{132}$** and **W${}_{12}$** by electrostatic connections and the occupied areas of the surfactant increased with the increasing distance away from the cluster cores (Fig. 1 and S1). Therefore, the surfactant molecules were loosely attached to the surfaces of the clusters and thus indicative of highly interdigitated or titled behaviors in the solid states. This was consistent with the aforementioned much shorter spacings obtained from the SAXS measurements.

As shown in Fig. S18a, the obtained value of σ was 0.42 mS cm^{-1} for **W${}_{12}$-DB24C8** at 293 K, which was much smaller than the result of the supramolecular network of **W${}_{12}$-PCL** (5.2 mS cm^{-1}). However, it was really difficult to compress **Mo${}_{132}$-DB24C8** into thin slices because of the highly fragmented sample. Therefore, its proton conductivity was measured by using electrochemical impedance spectroscopy (EIS). The EIS was performed on an electrochemical workstation (CHI 660E, Shanghai Chenhua) with a three-electrode system, where a platinum wire, Ag/AgCl (3 M KCl), and glassy carbon electrodes (GCE, *d* = 3 mm, catalyst loading: 0.285 mg cm^2) were used as the counter, reference, and working electrodes, respectively. The ethanol dispersion of **Mo${}_{132}$-DB24C8** were cast onto the working electrode and further dried under an infrared lamp. For the EIS measurement, the scanning frequency ranged from 0.1 Hz to 100 kHz. The experimental result showed that the proton conductivity was very poor for **Mo${}_{132}$-DB24C8** (Fig. S18b). These results displayed that the observed conductivities arose definitely from the supramolecular networks of **Mo${}_{132}$-PCL** and **W${}_{12}$-PCL**.

References

S1 D.-J. Feng, X.-Q. Li, X.-Z. Wang, X.-K. Jiang and Z.-T. Li, *Tetrahedron*, 2004, **60**, 6137.

S2 (*a*) Z. Ge, J. Hu, F. Huang and S. Liu, *Angew. Chem. Int. Ed.*, 2009, **48**, 1798; (*b*) L. Li, Y. Cong, L. He, Y. Wang, J. Wang, F.-M. Zhang and W. Bu, *Polym. Chem.,* 2016, **7**, 6288.

S3 D. Volkmer, A. Du Chesne, D. G. Kurth, H. Schnablegger, P. Lehmann, M. J. Koop and A. Müller, *J. Am. Chem. Soc.* 2000, **122***, 1995.*

Additional references for the molecular design and synthesis of secondary dialkylammonium salt/crown ether [2]pseudorotaxanes.

S4 (*a*) S. J. Cantrill, G. J. Youn and J. F. Stoddart, *J. Org. Chem.,* 2001, **66**, 6857; (*b*) Q.-S. Zong, C. Zhang and C.-F. Chen, *Org. Lett.*, 2006, **8**, 1859; (*c*) C. Zhang, S. Li, J. Zhang, K. Zhu, N. Li and F. Huang, *Org. Lett.*, 2007, **9**, 5553; (*d*) H. W. Gibson, N. Yamaguchi and J. W. Jones*, J. Am. Chem. Soc.,* 2003, **125**, 3522; (*e*) B. Yu, B. Wang, S. Guo, Q. Zhang, X. Zheng, H. Lei, W. Liu, W. Bu, Y. Zhang and X. Chen, *Chem. Eur. J.*, 2013, **19**, 4922; (*f*) L. He, J. Liang, Y. Cong, X. Chen and W. Bu, *Chem. Commun.,* 2014, **50**, 10841; (*g*) S. J. Cantrill, D. A. Fulton, A. M. Heiss, A. R. Pease, J. F. Stoddart, A. J. P. White and D. J. Williams, *Chem. Eur. J.*, 2000, **6**, 2274.

S5 (*a*) L. Chen, Y.-K. Tian, Y. Ding, Y.-J. Tian and F. Wang, *Macromolecules*, 2012, **45**, 8412; (*b*) D. Liu, D. Wang, M. Wang, Y. Zheng, K. Koynov, G. K. Auernhammer, H.-J. Butt and T. Ikeda, *Macromolecules*, 2013, **46**, 4617; (*c*) H. Li, X. Fan, W. Tian, H. Zhang, W. Zhang and Z. Yang, *Chem. Commun.*, 2014, **50**, 14666; (*d*) L. Li, Y. Cong, L. He, Y. Wang, J. Wang, F.-M. Zhang and W. Bu, *Polym. Chem.*, 2016, **7**, 6288; (*e*) F. Zeng, Y. Shen and C.-F. Chen, *Soft Matter*, 2013, **9**, 4875; (*f*) S. Li, H.-Y. Lu, Y. Shen and C.-F. Chen, *Macromol. Chem. Phys.*, 2013, **214**, 1596.